

Comparative Reactivity of Triruthenium and Triosmium $\mu_3\text{-}\eta^2$ -Imidoys. 2. Reactions with Alkynes

Shariff E. Kabir and Edward Rosenberg*

Department of Chemistry, The University of Montana, Missoula, Montana 59812

Luciano Milone, Roberto Gobetto, Domenico Osella, and Mauro Ravera

Dipartimento di Chimica IFM, Università di Torino, 10125 Torino, Italy

Timothy McPhillips, Michael W. Day, Douglas Carlot, Sharad Hajela,
Erich Wolf, and Kenneth Hardcastle

Department of Chemistry, California State University, Northridge, California 91330

Received December 23, 1996[®]

The reactions of $\text{Ru}_3(\text{CO})_9(\mu_3\text{-}\eta^2\text{-CH}_3\text{C}=\text{NCH}_2\text{CH}_3)(\mu\text{-H})$ (**1**), $\text{M}_3(\text{CO})_9(\mu_3\text{-}\eta^2\text{-C}=\text{N}(\text{CH}_2)_3)(\mu\text{-H})$ ($\text{M} = \text{Ru}$ (**2**), $\text{M} = \text{Os}$ (**3**)) with the alkynes $\text{RC}\equiv\text{CR}$ ($\text{R} = \text{CH}_3$, C_6H_5 , CO_2Me) have been studied. The ruthenium complexes **1** and **2** react with 2-butyne at 70 °C to give two very different trimetallic alkyne derivatives: $\text{Ru}_3(\text{CO})_7(\mu\text{-}\eta^2\text{-}\eta^4\text{-C}_4(\text{CH}_3)_4)(\mu\text{-}\eta^2\text{-CH}_3\text{C}=\text{NCH}_2\text{CH}_3)(\eta^1\text{-COC}(\text{CH}_3)\text{C}(\text{H})\text{CH}_3)$ (**5**) and $\text{Ru}_3(\text{CO})_8(\mu_3\text{-}\eta^2\text{-C}=\text{N}(\text{CH}_2)_3)(\mu\text{-}\eta^2\text{-CH}_3\text{C}(\text{H})=\text{CCH}_3)$ (**6**). The osmium imidoyl **3** does not react with 2-butyne even at elevated temperatures. However, the reaction of $\text{Os}_3(\text{CO})_9(\mu\text{-}\eta^2\text{-C}=\text{N}(\text{CH}_2)_3)(\mu\text{-H})(\text{CH}_3\text{CN})$ (**7b**), synthesized from $\text{Os}_3(\text{CO})_{10}(\mu\text{-}\eta^2\text{-C}=\text{N}(\text{CH}_2)_3)(\mu\text{-H})$ (**7a**), with 2-butyne yields the analog of **6**, $\text{Os}_3(\text{CO})_8(\mu_3\text{-}\eta^2\text{-C}=\text{N}(\text{CH}_2)_3)(\mu\text{-}\eta^2\text{-RC}(\text{H})=\text{CR})$ ($\text{R} = \text{CH}_3$ (**10**), $\text{R} = \text{C}_6\text{H}_5$ (**11**)) on thermolysis of the initially formed nonacarbonyl precursors (**8** and **9** for $\text{R} = \text{CH}_3$), which are a mixture of isomers. Direct reaction of **7a** with diphenylacetylene at 100 °C gives somewhat lower yields of **11**. The reaction of **7b** with dimethylacetylenedicarboxylate or the direct reaction of **3** with this alkyne yields the nonacarbonyl derivative $\text{Os}_3(\text{CO})_9(\mu\text{-}\eta^2\text{-C}=\text{N}(\text{CH}_2)_3)(\mu_3\text{-}\eta^3\text{-CH}_3\text{O}_2\text{CC}=\text{C}(\text{H})\text{CO}_2\text{CH}_3)$ (**12**). Direct reaction of **7a** with a 2.5 molar excess trimethylamine *N*-oxide at room temperature yields the alkyne–imidoyl-coupled product $\text{Os}_3(\text{CO})_8(\mu\text{-}\eta^6\text{-CH}_3\text{C}(\text{H})=\text{C}(\text{CH}_3)\text{C}(\text{CH}_3)=\text{C}(\text{CH}_3)\text{C}=\text{N}(\text{CH}_2)_3)$ (**13**). The solid state structures of **5**, **11**, **12**, and **13** are reported. A comparative study of the electrochemical properties of **5** and **1** is also reported.

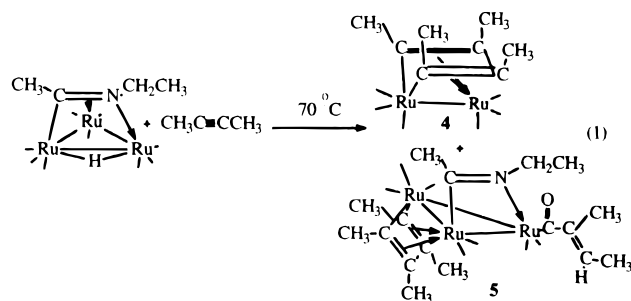
Introduction

In previous papers, we and others have reported the reactions of $\mu_3\text{-}\eta^2$ -imidoyl clusters with CO, PPh_3 , and MeNC .^{1–3} In addition to the expected greater reactivity of the triruthenium derivatives relative to their osmium analogs, we also observed a remarkable sensitivity to the substituent on the nitrogen atom in the observed structures of the products and on the mechanisms of the reported dynamical processes for both metals. Given the previously reported reactivity of triruthenium clusters containing nitrogen heterocycles toward alkynes⁴ and the activity of the resulting alkyne derivatives as hydrogenation catalysts,⁵ we thought it would be useful

to perform a similar study of the reactions of alkynes with the $\mu_3\text{-}\eta^2$ -imidoyl clusters of ruthenium and osmium. We report here the results of these investigations, with $\text{Ru}_3(\text{CO})_9(\mu_3\text{-}\eta^2\text{-CH}_3\text{C}=\text{NCH}_2\text{CH}_3)(\mu\text{-H})$ (**1**) and $\text{M}_3(\text{CO})_9(\mu_3\text{-}\eta^2\text{-C}=\text{N}(\text{CH}_2)_3)(\mu\text{-H})$ ($\text{M} = \text{Ru}$, **2**; $\text{M} = \text{Os}$, **3**), where we observe an even greater variety in reactivity and structural type for related osmium and ruthenium systems than that observed with other ligands.

Results and Discussion

A. Reactions of Triruthenium and Triosmium $\mu_3\text{-}\eta^2$ -Imidoys with Alkynes. The reaction of **1** with 2-butyne at 70 °C leads to a complex mixture of products, two of which can be isolated in sufficient amounts to be fully characterized, $\text{Ru}_2(\text{CO})_6(\mu\text{-}\eta^4\text{-C}_4(\text{CH}_3)_4)$ (**4**) and $\text{Ru}_3(\text{CO})_7(\mu\text{-}\eta^2\text{-}\eta^4\text{-C}_4(\text{CH}_3)_4)(\mu\text{-}\eta^2\text{-CH}_3\text{C}=\text{NCH}_2\text{CH}_3)(\eta^1\text{-COC}(\text{CH}_3)\text{C}(\text{H})\text{CH}_3)$ (**5**, eq 1). The solid



state structure of **5** is shown in Figure 1, crystal data

[®] Abstract published in *Advance ACS Abstracts*, May 15, 1997.
(1) See previous paper and the reference listed below: (a) Gobetto, R.; Hardcastle, K. I.; Kabir, S. E.; Milone, L.; Nishimura, N.; Botta, M.; Rosenberg, E.; Yin, M. *Organometallics* **1995**, *14*, 3068 and references cited therein. (b) Süß-Fink, G.; Jenke, T.; Heitz, H.; Pellinghelli, M. A.; Tiripicchio, A. *J. Organomet. Chem.* **1989**, *379*, 311. (c) Pellinghelli, M. A.; Tiripicchio, A.; Cabeza, J. A.; Oro, L. A. *J. Chem. Soc., Dalton Trans.* **1990**, 1509. (d) Rosenberg, E.; Kabir, S. E.; Day, M.; Hardcastle, K. I.; Irving, M. *J. Cluster Sci.* **1994**, *5*, 481. (e) Bruce, M. I.; Wallis, R. C. *Aust. J. Chem.* **1982**, *35*, 709. (f) Basu, A.; Bhaduri, S.; Sharma, K.; Jones, P. G.; Carpenter, G. *J. Chem. Soc., Dalton Trans.* **1990**, 1305. (g) Eisenstadt, A.; Giandomenico, C. M.; Frederick, M. F.; Laine, R. M. *Organometallics* **1985**, *4*, 2033. (h) Fish, R. H.; Kim, T. J.; Stewart, J. L.; Bushweller, J. H.; Rosen, R. K.; Dupon, J. W. *Organometallics* **1986**, *5*, 2193. (i) Casey, C. P.; Widenhoefer, R. A.; Hallenbeck, S. L.; Hayashi, R. K.; Gavney, J. A. *Organometallics* **1994**, *13*, 4720. (j) McKenna, S. T.; Andersen, R. A.; Muettterties, E. L. *Organometallics* **1986**, *5*, 2233.
(2) Day, M.; Espitia, D.; Hardcastle, K. I.; Kabir, S. E.; Rosenberg, E.; Gobetto, R.; Milone, L.; Osella, D. *Organometallics* **1991**, *10*, 3550.
(3) Day, M.; Espitia, D.; Hardcastle, K. I.; Kabir, S. E.; McPhillips, T.; Rosenberg, E.; Gobetto, R.; Milone, L.; Osella, D. *Organometallics* **1993**, *12*, 2304.

Table 1. Crystal Data for **5**, **11**, **12**, and **13**

	5	11	12	13
empirical formula	C ₂₄ H ₂₇ NO ₈ Ru ₃	C ₂₆ H ₁₇ NO ₈ Os ₃	C ₁₉ H ₁₃ NO ₁₃ Os ₃	C ₂₀ H ₁₉ NO ₈ Os ₃
fw	760.68	1042.03	1033.90	971.97
temperature, K	293(2)	293(2)	293(2)	293(2)
wavelength, Å	0.710 73	0.710 73	0.710 73	0.710 73
cryst syst	triclinic	monoclinic	monoclinic	monoclinic
space group	$P\bar{1}$	$P2_1/n$	$P2_1/n$	$P2_1/n$
<i>a</i> , Å; α , deg	9.141(2); 93.24(3)	12.227(2); 90	10.561(2); 90	8.916(1); 90
<i>b</i> , Å; β , deg	9.139(2); 95.42(3)	16.659(2); 100.90(2)	20.688(4); 90.31(3)	22.359(5); 95.65(1)
<i>c</i> , Å; γ , deg	18.848(4); 115.44(3)	13.464(3); 90	11.336(2); 90	12.078(2); 90
volume, Å ³ ; <i>Z</i>	1407.2(5); 2	2693(2); 4	2476.6(9); 4	2395(3); 4
density (calcd), g/cm ³	1.795	2.57	2.770	2.69
abs coeff, cm ⁻¹	16.33	141.9	154.19	159.4
<i>F</i> (000)	748	1888.0	1860	1748
crystal size, mm ³	0.5 × 0.05 × 0.5	0.30 × 0.30 × 0.40	0.60 × 0.45 × 0.40	0.10 × 0.07 × 0.27
θ range for data collection, deg	1.09–26.97	2.0–23.0	1.97–26.79	2.0–23.0
limiting indices	$-11 \leq h \leq 11, -10 \leq k \leq 10, -22 \leq l \leq 22$	$-13 \leq h \leq 13, 0 \leq k \leq 18, -14 \leq l \leq 14$	$-12 \leq h \leq 12, -24 \leq k \leq 24, -13 \leq l \leq 13$	$-9 \leq h \leq 9, 0 \leq k \leq 24, -13 \leq l \leq 13$
abs corr	ψ	ψ	ψ	ψ
no. of reflns collected	12214	8480	17470	7184
no. of independent reflns	6107 ($R_{\text{int}} = 0.023$)	4078 ($R_{\text{int}} = 0.050$)	4372 ($R_{\text{int}} = 0.090$)	3435 ($R_{\text{int}} = 0.029$)
refinement method	full-matrix least-squares on F^2	full-matrix least-squares on F^2	full-matrix least-squares on F^2	full-matrix least squares on F^2
data/restraints/parameters	6107/0/316	2706/0/343	4372/0/325	3435/0/289
goodness-of-fit on F^2	1.719	0.90	1.187	0.96
final <i>R</i> indices [$I > 2\sigma(I)$]	$R_1 = 0.0462, wR_2 = 0.0802$	$R_1 = 0.0257, wR_2 = 0.0307$	$R_1 = 0.0427, wR_2 = 0.0879$	$R_1 = 0.0300, wR_2 = 0.0334$
<i>R</i> indices (all data) ^a	$R_1 = 0.0643, wR_2 = 0.0733$		$R_1 = 0.0544, wR_2 = 0.0926$	
largest diff peak and hole, e Å ⁻³	0.936 and -0.767	0.48(18)	1.783 and -1.564	0.74(20)

^a Not available for compounds **11** and **13**.

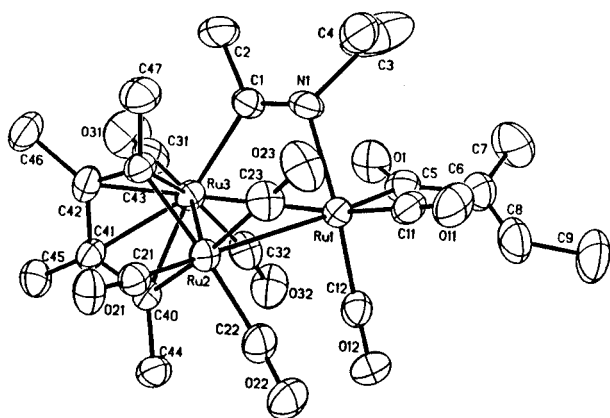


Figure 1. Solid state structure of **5**.

are given in Table 1, and selected distances and bond angles are given in Table 2. The structure of **5** consists of an Ru₃ triangle with a $\mu\text{-}\eta^2$ -imido ligand bridging the Ru(1)–Ru(3) edge, a metalocyclopentadienyl moiety containing Ru(2) and $\eta^4\text{-}\pi$ -bound to Ru(3), and an η^1 -vinyl acyl attached to Ru(1). The Ru(1)–Ru(2) bond length of 3.073(1) Å is extremely long, but is a required metal–metal bond considering that **5** is a 48e⁻ cluster. As expected, the μ -imido carbon–nitrogen bond is shortened (1.255(2) Å) relative to the triruthenium μ_3 -imidoyls previously reported.^{6–8} The imido carbon–Ru(3) and the N–Ru(1) bonds are also somewhat elongated relative to those in the phosphine-substituted derivatives of **1**.^{1,6} The Ru(1)–C(5) bond is typical for η^1 -ruthenium acyls,⁹ and the carbon–carbon bond (C(5)–C(6) = 1.476(9) Å) is elongated with respect to that

Table 2. Selected Distances (Å) and Angles (deg) for **5**^a

Distances			
Ru(1)–Ru(2)	3.073(1)	C(1)–N(1)	1.255(2)
Ru(1)–Ru(3)	2.897(1)	C(5)–O(1)	1.202(7)
Ru(2)–Ru(3)	2.780(2)	C(5)–C(6)	1.476(9)
Ru(3)–C(1)	2.082(6)	C(40)–C(41)	1.388(7)
Ru(1)–N(1)	2.081(5)	C(41)–C(42)	1.450(8)
Ru(1)–C(5)	2.032(7)	C(42)–C(43)	1.374(8)
Ru(2)–C(40)	2.053(6)	C–O ^b	1.153(7)
Ru(2)–C(43)	2.060(6)		
Ru(3)–C(40)	2.259(6)		
Ru(3)–C(41)	2.240(6)		
Ru(3)–C(42)	2.252(6)		
Ru(3)–C(43)	2.254(6)		
Ru–CO ^b	1.859(7)		

Angles			
Ru(1)–Ru(2)–Ru(3)	59.07(3)	C(2)–C(1)–N(1)	121.1(5)
Ru(1)–Ru(2)–Ru(3)	59.07(3)	C(1)–N(1)–C(3)	124.9(5)
Ru(1)–Ru(3)–Ru(2)	65.52(3)	O(1)–C(5)–C(6)	118.7(7)
Ru(21)–Ru(1)–Ru(3)	55.41(3)	C(5)–C(6)–C(2)	117.1(7)
Ru(21)–Ru(1)–Ru(3)	55.41(3)	C(40)–C(41)–C(42)	112.3(5)
C(1)–Ru(3)–Ru(2)	98.8(2)	C(41)–C(42)–C(43)	116.0(5)
N(1)–Ru(1)–Ru(2)	90.9(2)	Ru–C–O ^b	176.0(7)
C(5)–Ru(1)–Ru(2)	110.0(2)		

^a Numbers in parentheses are estimated standard deviations.

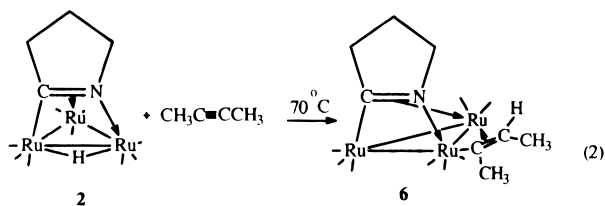
^b Average values.

expected for an uncoordinated double bond. The intraligand distances for the metalocyclopentadienyl group are typical for related compounds such as direct analogs of **4**.¹⁰ The ¹H-NMR of **5** in solution is entirely consistent with the solid state structure. Six singlet methyl resonances are observed in the range 2.0–2.5 ppm, and one methyl doublet at 1.95 ppm which is coupled to a quartet at 6.35 ppm is assignable to the vinylic hydrogen. The methylene resonances of the ethyl group appear as the expected pair of AB multiplets at 3.91 and 3.61 ppm and are coupled to a triplet at 1.12 ppm.

In sharp contrast to the results obtained from the reaction of **1** with 2-butyne, compound **2** reacts with 2-butyne to give one compound, Ru₃(CO)₈($\mu_3\text{-}\eta^2\text{-C}\equiv\text{N}(\text{CH}_2)_3(\mu\text{-}\eta^2\text{-CH}_3\text{CC}(\text{H})\text{CH}_3)$ (**6**, eq 2),

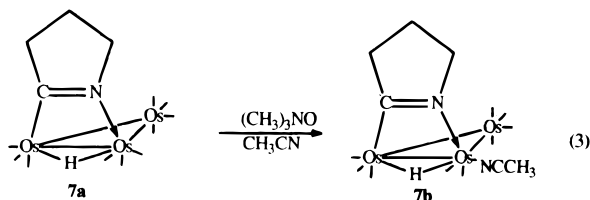
(4) (a) Cabeza, J. A.; Fernandez-Colinas, J. M.; Llamazares, A.; Riera, V.; Garcia-Grande, S.; Van der Maelen, J. F. *Organometallics* **1994**, *13*, 4352. (b) Lugan, N.; Laurent, F.; Lavigne, G.; Newcomb, T. P.; Llimatta, E. W.; Bonnet, J. *J. Am. Chem. Soc.* **1990**, *112*, 8607. (c) Nombel, P.; Lugan, N.; Mulla, F.; Lavigne, G. *Organometallics* **1994**, *13*, 4673.

(5) Cabeza, J. A.; del Rio, I.; Fernandez-Colinas, J. M.; Riera, V. *Organometallics* **1996**, *15*, 449.

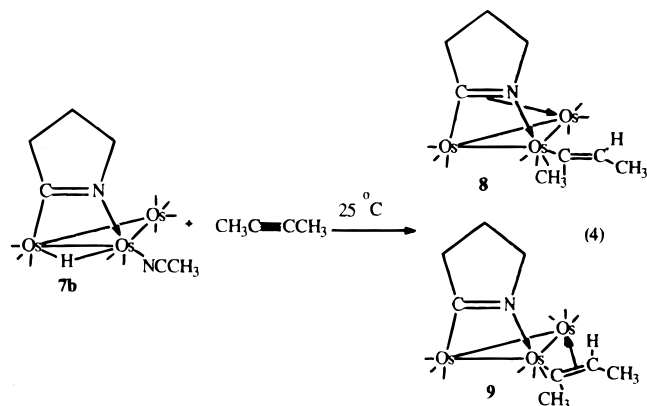


whose structure is assigned on the basis of spectroscopic evidence and by analogy with closely related triruthenium 2-amino-6-methylpyridine complexes^{4,5} and with the osmium analogs presented below. As for the reactions of **1** and **2** with phosphines, the presence of the ethyl group in **1** significantly alters the course of the reaction relative to the less sterically encumbered μ_3 - η^2 -imido **2**. One can visualize initial formation of an analog of **6** which then converts to an η^1 -vinyl acyl to relieve steric crowding. This, in turn, would create multiple vacant coordination sites which could then react further with alkyne to form **5** and perhaps fragment to form **4**.

Compound **3** does not react with 2-butyne at all even at elevated temperatures. It does react with less volatile alkynes but only at 100 °C (*vide infra*). Thus, the triosmium imido complexes are less reactive toward alkynes than their triruthenium analogs.¹ We recently reported that the decacarbonyl precursor to **3**, $\text{Os}_3(\text{CO})_{10}(\mu\text{-}\eta^2\text{-C=N}(\text{CH}_2)_3)(\mu\text{-H})(\mathbf{7a})$ undergoes reaction with trimethylamine *N*-oxide in acetonitrile/methylene chloride regioselectively (eq 3).¹¹ The resulting acetonitrile de-



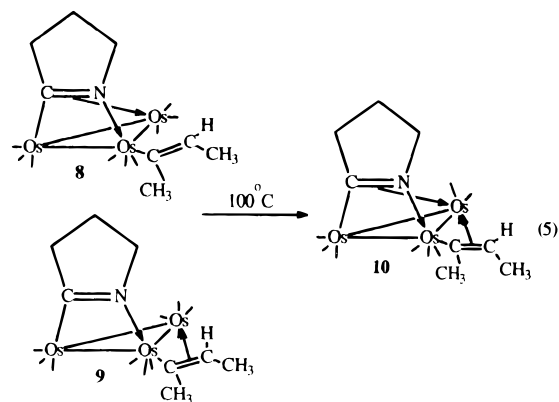
rivative $\text{Os}_3(\text{CO})_9(\mu\text{-}\eta^2\text{-C=N}(\text{CH}_2)_3)(\mu\text{-H})(\text{CH}_3\text{CN})(\mathbf{7b})$ does react smoothly with $\text{C}_2(\text{CH}_3)_2$ at ambient temperatures to give a single product band on purification by thin layer chromatography which proved to be an inseparable mixture of isomers. On the basis of the ¹H-NMR data, we can tentatively assign the structures which comprise this mixture to two major types: $\text{Os}_3(\text{CO})_9(\mu_3\text{-}\eta^2\text{-C=N}(\text{CH}_2)_3)(\eta^1\text{-CH}_3\text{C=C}(\text{H})\text{CH}_3)(\mathbf{8})$ and $\text{Os}_3(\text{CO})_9(\mu\text{-}\eta^2\text{-C=N}(\text{CH}_2)_3)(\mu\text{-}\eta^2\text{-CH}_3\text{C=C}(\text{H})\text{CH}_3)(\mathbf{9})$, (eq 4).



These assignments are based on the observation of two different quartet resonances at 3.93 and 6.90 ppm which are coupled to two different methyl group doublets at 2.58 and 2.10 ppm, respectively. Two singlet methyl

resonances of the same relative intensity as the doublet methyl resonances are also observed at 2.99 and 2.29 ppm. Complexation of the vinyl group in a $\mu\text{-}\eta^2\text{-}\sigma\text{-}\pi$ bonding mode leads to an upfield shift of the vinyl hydrogen while the η^1 -vinyl hydrogen would be expected to be found downfield. The ¹H-NMR data for the vinylic hydrogens in **5** and **6** illustrate this trend nicely (6.35 and 2.16 ppm, respectively). Further evidence for the proposed structures of **8** and **9** comes from the ¹³C-NMR of the mixture which shows four resonances assignable to the C=N carbons at 216.33, 213.13, 212.14, and 189.86 ppm in a relative intensity of 1:0.3:0.8:0.2. The three most downfield resonances can be assigned to π -complexed imido carbons in the three possible isomers of **8** since these are usually found in the range 210–220 ppm in related complexes.¹ The resonance at 189.86 ppm can be assigned to the imido carbon in **9** since this type of resonance is found in the 190–200 ppm range (this type of carbon is observed at ~198 ppm in **12**, reported below).¹ Two well-resolved CH resonances are also observed at 112.79 and 94.57 ppm, which can be assigned to vinylic resonances in **8** (the π -complexed vinylic CH in **10** reported below comes at 77.27 ppm). In addition, the presence of minor isomers is also evident in the ¹H-NMR from the presence of lower intensity methyl singlets, doublets, and methylene multiplets. This spectral complexity of the isomeric mixture of **8** and **9** is attributable to the presence of conformers for **9** where the associated vinyl hydrogen quartets overlap with other ligand resonances. We cannot exclude the possibility that the lower intensity signals observed are due to other types of isomers which differ by the location of vinyl group on the osmium triangle or even binuclear species. Variable-temperature studies to see if **8** and **9** are in equilibrium were precluded by their conversion to **10** on heating (see below).

Thermolysis of the mixture of **8** and **9** at 100 °C results in conversion to a single product $\text{Os}_3(\text{CO})_8(\mu_3\text{-}\eta^2\text{-C=N}(\text{CH}_2)_3)(\mu\text{-}\eta^2\text{-CH}_3\text{C=C}(\text{H})\text{CH}_3)(\mathbf{10})$, (eq 5). Com-



pound **10** was characterized spectroscopically and by elemental analysis. A similar mixture of isomers to that found in the reaction of 2-butyne with **7b** is isolated from the reaction of **7b** with diphenylacetylene at ambient temperatures. On thermolysis this mixture gives one compound, $\text{Os}_3(\text{CO})_8(\mu_3\text{-}\eta^2\text{-C=N}(\text{CH}_2)_3)(\mu\text{-}\eta^2\text{-C}_6\text{H}_5\text{C=C}(\text{H})\text{C}_6\text{H}_5)(\mathbf{11})$. Compound **11** is also obtained in moderate yield by direct reaction of **3** with diphenylacetylene in refluxing heptane. Compound **11** was characterized spectroscopically and by a solid state structural investigation. The solid state structure of **11**

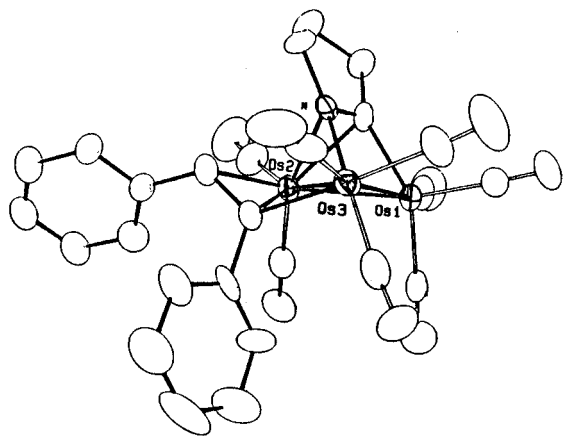


Figure 2. Solid state structure of **11**.

Table 3. Selected Distances (Å) and Bond Angles (deg) for **11**^a

Distances			
Os(1)–Os(2)	2.7067(7)	C(1)–N	1.36(2)
Os(1)–Os(3)	2.8939(7)	C(5)–C(6)	1.45(2)
Os(2)–Os(3)	2.7106(6)	C(4)–N	1.50(2)
Os(1)–C(1)	2.06(1)	C(1)–C(2)	1.54(2)
Os(2)–N	2.17(1)	C(2)–C(3)	1.55(2)
Os(2)–C(1)	2.30(1)	C(3)–C(4)	1.55(2)
Os(3)–N	2.14(1)	C(5)–C(51)	1.52(2)
Os(2)–C(5)	2.16(1)	C(6)–C(61)	1.49(2)
Os(2)–C(6)	2.31(1)	C–O ^b	1.14(2)
Os(3)–C(5)	2.17(1)		
Os–CO ^b	1.91(1)		

Angles			
Os(1)–Os(2)–Os(3)	64.58(2)	N–C(1)–C(2)	111(1)
Os(1)–Os(3)–Os(2)	57.64(2)	C(1)–N–C(4)	112(1)
Os(2)–Os(1)–Os(3)	57.78(3)	C(5)–C(6)–C(61)	124(1)
Os(3)–Os(2)–N	50.6(2)	C(6)–C(5)–C(51)	120(1)
Os(1)–Os(2)–C(1)	47.8(3)		
Os(3)–Os(2)–C(6)	77.0(3)		
Os(2)–C(5)–Os(3)	77.6(4)		
Os–C–O ^b	177(1)		

^a Numbers in parentheses are estimated standard deviations.

^b Average values.

is shown in Figure 2, crystal data are given in Table 1, and selected distances and bond angles are given in Table 3. Compound **11** consists of an isosceles triangle of osmium atoms with a μ_3 -imidoyl ligand bridging the elongated Os(1)–Os(3) edge and the carbon–nitrogen double bond being coordinated to Os(2). The σ - π -vinyl ligand bridges the Os(2)–Os(3) edge which is virtually identical in length with the Os(1)–Os(3) edge. The geometry of the μ_3 -imidoyl ligand is distinctly different from related face-capping imidoyls in that the Os(3)–N and Os(2)–N bond lengths are almost equal, being 2.14(1) and 2.17(1) Å, respectively.^{1–3} The Os(1) and C(1) and Os(2) and C(1) distances are more typical at 2.06(1) and 2.30(1) Å, respectively. The corresponding bond lengths in **3** are 2.08(1) and 2.30(1) Å.³ The Os(2)–C(5) and Os(3)–C(5) vectors are also almost equal

(6) (a) Hansert, B.; Tasi, M.; Tiripicchio, A.; Tiripicchio-Camellini, M.; Vahrenkamp, H. *Organometallics* **1991**, *10*, 4070. (b) Basu, A.; Bhaduri, S.; Sharma, K.; Jones, P. G. *J. Chem. Soc., Chem. Commun.* **1987**, 1126.

(7) Aime, S.; Gobetto, R.; Padovan, F.; Botta, M.; Rosenberg, E.; Gellert, R. W. *Organometallics* **1987**, *6*, 2074.

(8) Day, M. W.; Hajela, S.; Kabir, S. E.; Irving, M.; McPhillips, T.; Wolf, E.; Hardcastle, K. I.; Rosenberg, E.; Milone, L.; Gobetto, R.; Osella, D. *Organometallics* **1991**, *10*, 2743.

(9) Mayr, A.; Lin, Y. C.; Boag, N. M.; Kaesz, H. D. *Inorg. Chem.* **1982**, *21*, 1704.

(10) Osella, D.; Arman, G.; Gobetto, R.; Laschi, F.; Zanello, P.; Ayrton, S.; Goodfellow, V.; Housecroft, C. E.; Owen, S. M. *Organometallics* **1989**, *8*, 2689 and references therein.

(11) Rosenberg, E.; Kabir, S. E.; Day, M.; Hardcastle, K. I.; Wolf, E.; McPhillips, T. *Organometallics* **1995**, *14*, 721.

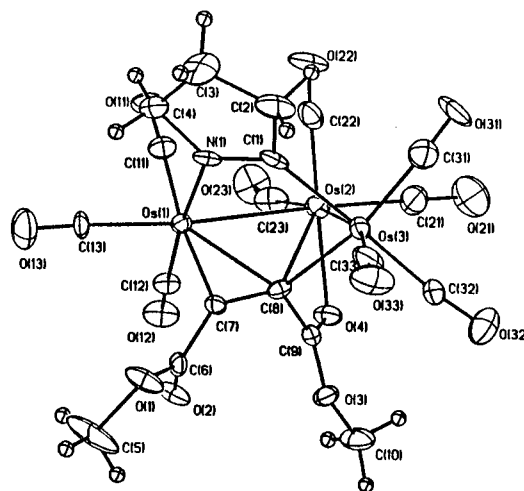
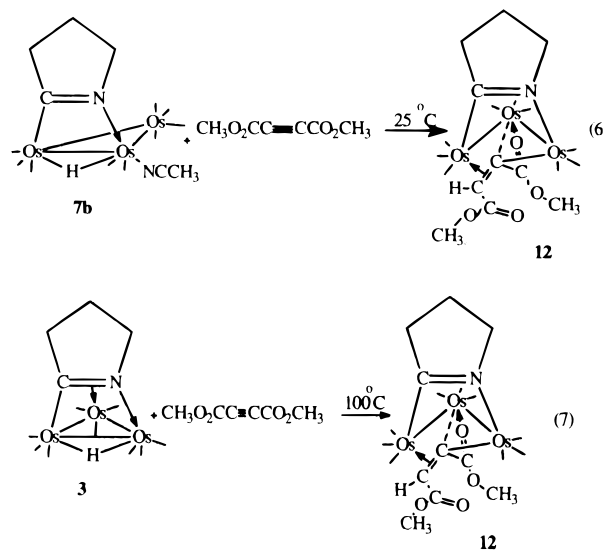


Figure 3. Solid state structure of **12**.

in length at 2.16(1) and 2.17(1) Å, while the Os(2)–C(6) bond length is considerably longer at 2.31(1) Å. This overall disposition results in an effective π -interaction with Os(2) and σ -interaction with Os(3). This type of bonding mode is well documented for the alkyne derivatives of the triruthenium $\mu_3\text{-}\eta^2$ -2-amino-6-methylpyridine clusters,^{4,5} but **10** and **11** are the first triosmium clusters with both σ - π -vinyl and a face-capping nitrogen heterocycle. The η^1 -vinyl coordination proposed for **8** has been suggested as an intermediate in the hydrogenation of alkynes catalyzed by the 2-amino-6-methylpyridine analogs of **11**.⁵

In the hope of stabilizing a nonacarbonyl complex of the types proposed for **8** and **9**, we reacted **7b** with the electron poor alkyne, $\text{C}_2(\text{CO}_2\text{CH}_3)_2$. In fact, an apparent nonacarbonyl cluster, $\text{Os}_3(\text{CO})_9(\mu\text{-}\eta^2\text{-C}=\text{N}(\text{CH}_2)_3)(\mu_3\text{-}\eta^3\text{-CH}_3\text{O}_2\text{C}=\text{C}(\text{H})\text{CO}_2\text{CH}_3)$ (**12**) was isolated as the only major product from the reaction of **7b** with this alkyne at ambient temperatures or from its reaction with **3** at 100 °C (eqs 6 and 7). However, the structure of **12**



proved to be quite different from that proposed for either **8** or **9**. The solid state structure of **12** is shown in Figure 3, crystal data are given in Table 1, and selected distances and angles are given in Table 4. Compound **12** is a $50e^-$ cluster with two unequal metal–metal bonds, Os(1)–Os(2) at 2.969(1) Å and Os(2)–Os(3) at 2.746(1) Å. The imidoyl ligand bridges the open metal–

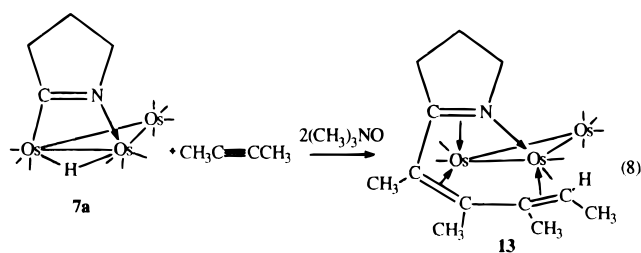
Table 4. Selected Distances (Å) and Angles (deg) for **12**^a

Distances			
Os(1)–Os(2)	2.969(1)	C(1)–N(1)	1.36(2)
Os(2)–Os(3)	2.746(1)	C(7)–C(8)	1.48(2)
Os(1)–N(1)	2.09(1)	C(9)–O(4)	1.91(1)
		C(6)–O(2)	1.24(2)
Os(3)–C(1)	2.22(1)	C(1)–C(2)	1.52(2)
Os(1)–C(7)	2.20(1)	C(2)–C(3)	1.58(2)
Os(1)–C(8)	2.39(1)	C(3)–C(4)	1.55(2)
Os(2)–C(8)	2.57(1)	C(4)–N(1)	1.54(2)
Os(3)–C(8)	2.10(1)	C(7)–C(6)	1.44(2)
Os–CO ^b	1.95(2)	C(8)–C(9)	1.56(2)
Os(2)–O(4)	2.16(2)	C–O ^b	1.11(2)
Angles			
Os(1)–Os(2)–Os(3)	82.08(2)	N(1)–Os(1)–C(8)	84.0(4)
Os(1)–Os(2)–O(4)	91.9(2)	N(1)–Os(1)–Os(2)	90.9(3)
N(1)–Os(1)–C(7)	81.3(4)	Os–C–O ^b	177(1)
Os(3)–Os(2)–C(8)	46.3(2)		

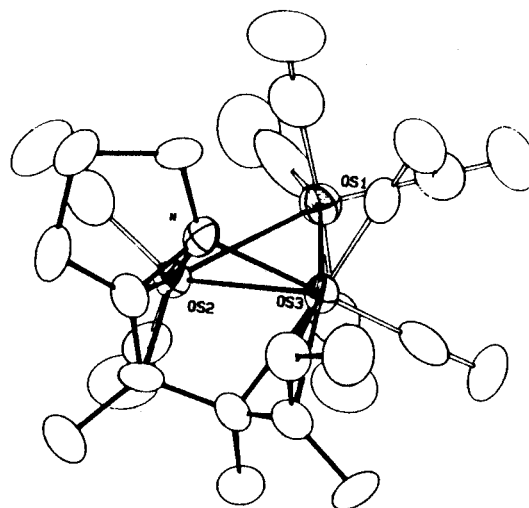
^a Numbers in parentheses are estimated standard deviations.^b Average values.

metal bond with Os(1)–N at 2.09(1) Å and Os(3)–C(1) at 2.22(1) Å. The latter is considerably elongated relative to other μ -imidoyls (2.06–2.10(1) Å) as might be expected since it is bridging a nonbonded metal vector. Each osmium atom is bound to three carbonyl groups, but Os(2) is also bound to the carbonyl oxygen of one of the carbomethoxy groups of the alkyne. The alkyne carbons C(7) and C(8) are π -bound to Os(1) with bond lengths that are fairly typical for such interactions at 2.20(1) and 2.39(1) Å.^{4,5} The Os(3)–C(8) bond length of 2.10(1) Å is typical for an osmium–carbon σ -bond while the Os(2)–C(8) at 2.57(1) Å must be considered a fairly weak interaction since it is nearly the sum of the covalent radii of these two elements (2.67 Å) and is very elongated compared with most osmium–carbon σ -bonds.^{1–5} In a general way **12** resembles the structure proposed for **9**, containing a μ - η^2 -imidoyl, a μ - η^2 -vinyl, and nine carbonyls. However, it is apparently the additional interaction with the organic carbonyl which makes **12** prefer this bonding mode over the μ_3 - η^2 -imidoyl and η^1 -vinyl and prevents **12** from existing as a complex mixture of isomers while stabilizing the noncarbonyl derivative. A similar carbonyl oxygen interaction accompanied by metal–metal bond rupture has been observed in dirhenium complexes of dicarbomethoxyacetylene.¹²

The compounds **9**–**12** show no tendency to react further with alkynes. Both straight thermal reactions and reactions in the presence of trimethylamine *N*-oxide failed to yield any new products, with nonspecific decomposition or recovery of starting material being the only reaction pathways observed. However, reaction of **7a** with 2 mol of trimethylamine *N*-oxide in the presence of 2-butyne at room temperature did result in the formation of Os₃(CO)₈(μ - η^6 -(CH₃C(H)=C(CH₃)C(CH₃)=C(CH₃)C=N(CH₂)₃) (13, eq 8) as well as considerable nonspecific decomposition.



Compound **13** was characterized by ¹H-NMR and infrared spectroscopy and by a single-crystal X-ray

**Figure 4.** Solid state structure of **13**.**Table 5.** Selected Distances (Å) and Bond Angles (deg) for **13**^a

Distances			
Os(1)–Os(2)	2.730(1)	C(4)–N(1)	1.43(2)
Os(1)–Os(3)	2.889(1)	C(4)–C(40)	1.38(2)
Os(2)–Os(3)	2.846(1)	C(40)–C(42)	1.52(2)
Os(2)–N	2.15(1)	C(42)–C(44)	1.49(2)
Os(2)–C(4)	2.21(1)	C(44)–C(46)	1.41(2)
Os(2)–C(40)	2.26(1)	N(1)–C(1)	1.51(3)
Os(3)–C(42)	2.32(1)	C(1)–C(2)	1.57(2)
Os(3)–C(44)	2.24(1)	C(2)–C(3)	1.59(2)
Os(3)–C(46)	2.26(1)	C(3)–C(4)	1.52(2)
Os–C–O ^b	1.86(2)	C–O ^b	1.17(2)
Angles			
Os(1)–Os(2)–Os(3)	62.38(2)	C(1)–N–C(4)	110(1)
Os(1)–Os(3)–Os(2)	56.85(2)	N–C(4)–C(1)	111(1)
Os(2)–Os(1)–Os(3)	60.77(2)	N–C(4)–C(40)	118(1)
Os(3)–Os(2)–N	47.3(3)	C(4)–C(40)–C(42)	119(1)
Os(3)–Os(2)–C(4)	71.9(3)	C(42)–C(44)–C(46)	118(1)
Os(1)–Os(2)–C(40)	134(2)	C(44)–C(46)–C(47)	124(1)
Os(1)–Os(2)–C(42)	102.2		
C(44)–Os(3)–C(46)	36.4(5)		
Os–C–O ^b	177(1)		

^a Numbers in parentheses are estimated standard deviations.^b Average values.

diffraction study. The solid state structure of **13** is shown in Figure 4, crystal data are given in Table 1, and selected distances and angles are given in Table 5. The structure of **13** consists of an Os₃ triangle with four carbonyl groups on Os(1) and two carbonyl groups on Os(2) and Os(3). The Os(2)–Os(3) edge is bridged by a single organic ligand consisting of two coupled 2-butyne, one of which is joined to the pyrrolidine ring at the imidoyl carbon. The ligand is an eight-electron donor which essentially raps around the Os(2)–Os(3) edge. The carbon nitrogen double bond is considerably elongated (1.43(2) Å) relative to other π -coordinated imidoyls (~1.35 Å).^{1–3} The C(40)–Os(2) and C(42)–Os(3) bond lengths of 2.26(1) and 2.32(1) Å taken together with the C(40)–C(42) bond length of 1.52(2) indicate that the Os(2)–Os(3)–C(40)–C(42) is a dimetallacyclobutane. The C(44)–C(46) bond length of 1.41(2) and the associated Os(3)–C(46) and C(44)–Os(3) distances of 2.26(1) and 2.24(1) Å indicate that this vinyl fragment interacts only with Os(3). The N–Os(3) bond length of 2.10 Å is fairly typical for μ -imidoyls.^{1–5} Although the oligomerization of alkynes on clusters is fairly common,¹³ coupling to a nitrogen heterocycle is rare and is reminiscent of the ruthenium carbonyl catalyzed cou-

(12) Adams, R. D.; Huang, M. *Organometallics* **1995**, *14*, 2887.(13) Shore, N. E. *Chem. Rev.* **1988**, *88*, 1081.

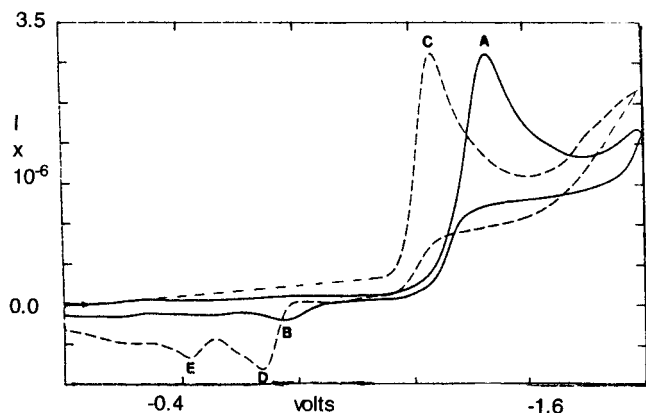


Figure 5. Cyclic voltammograms of **1** (solid line) and $\text{Ru}_3(\text{CO})_{10}(\mu\text{-}\eta^2\text{-CH}_3\text{C}=\text{NCH}_2\text{CH}_3)(\mu\text{-H})$ (dashed line) at 200 mV s^{-1} .

pling of olefins and carbon monoxide to pyridines to yield vinylacetylpyridines.¹⁴ The vinylic hydrogen on C(46) appears at a quartet at 1.75 ppm. This unusually high field chemical shift is probably the result of the observed orientation of the C(44)–C(46) vector which points this hydrogen directly at Os(3). The formation of **13** from the reaction of **7a** with 2 mol of trimethylamine *N*-oxide and 2-butyne but not from **9** and **12** suggests that multiple coordination sites must be simultaneously available for the observed coupling as was suggested for the formation of **5**.

B. Electrochemical Behavior of 1 and 5. Complex **5** represents an unusual example of a cluster containing three distinct organic moieties which are well-known as individual ligands but have never been observed together. The low yield obtained for **5** precluded detailed investigations of its chemistry, and we thought electrochemical measurements would provide an efficient means of making a preliminary probe of its electronic properties. For comparison, we have also investigated the electrochemical behavior of **1**.

The CV response of an acetone solution of **1** at a hanging mercury drop electrode (HMDE) is reported in Figure 5. The reduction process at peak A [$E_p(\text{A}) = -1.47 \text{ V}$] is chemically irreversible. In fact, no associated reoxidation peak could be found at scan rates as high as 1 V s^{-1} and at temperatures as low as $-20 \text{ }^\circ\text{C}$. In the reverse scan a small peak, B, is observed at -0.76 V , attributable to the reoxidation of fragment product(s). The breadth of the peak measured at the half-width ($E_p - E_{p/2}$) is 67 mV, close to $1e^-$ Nernstian behavior.¹⁰ The plot of i_p vs $V^{1/2}$ (the scan rate varying from 50 to 1000 mV s^{-1}) is linear through the origin, confirming the diffusion-controlled behavior.¹⁰ Besides this CV data, evidence of fast $1e^-$ transfer comes from the 65 mV slope¹⁰ of the plot of E vs $\log[(i_d - i)/i]$ obtained from the polarographic wave ($E^{1/2} = -1.43 \text{ V}$). The plot of E_p vs $\log v$ gives a slope of 38 mV, indicating the one-electron reduction is followed by a moderately fast, first-order chemical decomposition (EC mechanism). The polarographic response of an equimolar solution of **1** and ferrocene in acetone gives a current ratio equal to 0.9, confirming that wave A corresponds to a one-electron reduction process.

Bubbling CO into an acetone solution rapidly turns **1** into $\text{Ru}_3(\text{CO})_{10}(\mu\text{-}\eta^2\text{-CH}_3\text{C}=\text{NCH}_2\text{CH}_3)(\mu\text{-H})$. The CV

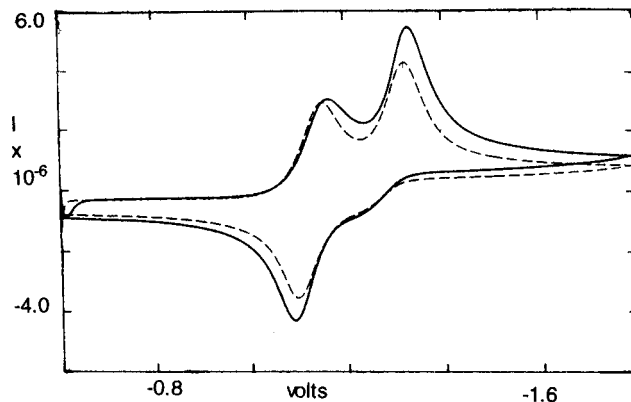


Figure 6. Cyclic voltammogram of **5** at 300 mV s^{-1} (solid line) and at 200 mV s^{-1} (dashed line).

response consists of a new $1e^-$ chemically irreversible reduction, peak C, at less negative potential [$E_p(\text{C}) = 1.28 \text{ V}$] followed in the reverse scan by two peaks, D and E, at -0.63 and -0.43 V , respectively, due to the reoxidation of fragments (Figure 5). All of the electrochemical features for the decacarbonyl are similar to those found for **1** and suggest an EC mechanism. By comparison of the polarographic $E_{1/2}$ values of **1** and the decacarbonyl, -1.43 and -1.24 V , respectively, it can be concluded that the addition of a further CO group which displaces the coordination of the C=N bond (originally present in **1**) decreases the electron density on the Ru_{13} triangle, making the reduction easier as would be expected from replacing the C=N bond π -coordination with a better π -acceptor ligand.

The electrochemical behavior of **5** is completely different from that of **1** or the corresponding decacarbonyl. The CV response of an acetone solution of **5** at an HMDE is shown in Figure 6. Two reduction peaks are observed at -1.17 and -1.33 V at a scan rate of 0.300 V s^{-1} . The $E_p - E_{p/2}$ values of 49 and 66 mV make these reduction waves close to $1e^-$ Nernstian behavior. The less cathodic values observed for these sequential $1e^-$ reductions clearly show that the site of reduction is different for **5** relative to **2**. Indeed, some related trinuclear complexes of the general formula $\text{M}_3(\text{CO})_8(\text{R}_2\text{C}_2)_2$ ($\text{M} = \text{Fe, Ru, Os}$; $\text{R} = \text{Me, Et, Ph}$) which have the $\mu\text{-}\eta^2\text{:}\eta^4$ -metallocyclopentadiene structure exhibit similar electrochemical behavior, having $1e^-$ reversible reductions in the range $1.16\text{--}1.42 \text{ V}$.¹⁰ It is reasonable that the more delocalized metallocyclopentadienyl moiety would have the lowest energy orbital for accepting electrons. Interestingly, the $\mu_3\text{-}\eta^4\text{-C}_4\text{R}_4$ clusters undergo only a $1e^-$ reversible reduction and then fragment to $\mu\text{-}\eta^4$ -dimetallic species, similar to **4**, upon accepting a second electron.¹⁰

Experimental Section

Compounds **1–3** were synthesized by known literature procedures.^{1f,2,3} All reactions were performed under an atmosphere of prepurified nitrogen, but were worked in the air. Thin layer chromatography was performed on 20×20 or $20 \times 40 \text{ cm}$ plates using a 1 mm layer of silica gel PF-254 (E&M Science). Methylene chloride was distilled from CaH_2 before use, and hexane was dried over sodium. Trimethylamine *N*-oxide (Aldrich) was dehydrated by distillation of the water–toluene azeotrope. Alkynes were purchased from Farchan and used as received. ^1H - and ^{13}C -NMR were obtained on a Bruker 360-AMX or a Varian 400 Unity Plus spectrometer. Infrared spectra were obtained on PE-1620 or 1400 spectrometers.

(14) Moore, E. J.; Pretzer, W. R.; O'Connell, T. J.; Harris, J.; LaBounty, L.; Chou, L.; Grimmer, S. S. *J. Am. Chem. Soc.* **1992**, *114*, 5888.

Elemental analyses were performed by Schwarzkopf Microanalytical Labs, New York.

Electrochemical Measurements. Voltammetric and polarographic measurements were performed with two sets of instrumentation: a PAR 273 electrochemical analyzer connected to an interfaced PC and an AMEL 553 potentiostat modulated by an AMEL 567 function generator and connected to an X–Y recorder.

A three-electron cell was designed to allow the tip of the reference electrode (SCE) to closely approach the working electrode. Compensation for the IR drop was applied through positive-feedback device. All measurements were carried out under nitrogen in anhydrous deoxygenated solvents. Solutions were 1×10^{-3} M for the compounds under study and 1×10^{-1} M for the supporting electrolyte, $[\text{Bu}_4\text{N}][\text{BF}_4]$. The temperature of the solution was kept constant (± 1 °C) by circulation of a thermostated water/ethanol mixture through a jacketed cell. The working electrode was a hanging mercury drop electrode (HMDE), or dropping mercury electrode (DME). Potential data (*vs* SCE) were checked against the ferrocene (0/1+) couple; under the actual experimental conditions, the ferrocene/ferrocenium couple is located at +0.51 V in acetone.

Reaction of 1 with 2-Butyne. **1** (400 mg, 0.64 mmol) was combined with 0.150 mL (1.9 mmol) 2-butyne and 250 mL of degassed hexane. The yellow solution was heated at reflux for 4 h. The dark red solution was filtered, rotary evaporated, taken up in methylene chloride, and purified by thin layer chromatography. Three major bands were eluted: the fastest moving band contained unreacted **1**, 22 mg, the second yellow band contained $\text{Ru}_2(\text{CO})_6[\eta^1\text{-}\eta^1\text{-}\eta^4\text{-}(\text{C}_4(\text{CH}_3)_4)]$ (**4**) (31 mg, 10%), and the third red band contained 32 mg (7%) of $\text{Ru}_3(\text{CO})_7(\mu\text{-}\eta^2\text{-}\eta^4\text{-}\text{C}_4(\text{CH}_3)_4)(\mu\text{-}\eta^2\text{-}\text{CH}_3\text{C}=\text{NCH}_2\text{CH}_3)(\eta^1\text{-}\text{COC}(\text{CH}_3)\text{C}(\text{H})\text{CH}_3)$ (**5**).

Analytical and Spectroscopic Data for 5. Anal. Calcd for $\text{C}_{24}\text{H}_{27}\text{O}_8\text{NRu}_3$: C, 37.89; H, 3.55; N, 1.84. Found: C, 37.06; H, 3.40; N, 1.89. IR ($\nu(\text{CO})$, C_6H_6): 2077 (m), 2041 (s), 2023 (s), 2008 (vs), 1988 (m, br), 1976 (m, br), 1968 (m, br) cm^{-1} . $^1\text{H-NMR}$ (CDCl_3 , 400 MHz): 6.35 (q, 1H), 3.91 (m, 1H), 3.61 (m, 1H), 2.51 (s, 3H), 2.43 (s, 3H), 2.29 (s, 3H), 2.11 (s, 3H), 2.04 (s, 3H), 1.95 (d, 3H), 1.83 (s, 3H), 1.12 (t, 3H) ppm.

Analytical and Spectroscopic Data for 4. Anal. Calcd for $\text{C}_{14}\text{H}_{12}\text{O}_6\text{Ru}_2$: C, 35.14; H, 2.50. Found: C, 35.81; H, 2.64. IR ($\nu(\text{CO})$, CH_2Cl_2) 2067 (m), 2034 (vs), 1998 (m, br), 1991 (m, br), 1971 (m, br) cm^{-1} . $^1\text{H-NMR}$ (CDCl_3 , 80 MHz): 2.37 (s, 6H), 2.21 (s, 6H) ppm.

Synthesis of $\text{Ru}_3(\text{CO})_8(\mu_3\text{-}\eta^2\text{-}\text{C}=\text{N}(\text{CH}_2)_3)(\mu\text{-}\eta^2\text{-}\text{CH}_3\text{C}=\text{C}(\text{H})(\text{CH}_3))$ (6**).** **2** (25 mg, 0.04 mmole) was combined with 50 mL of hexane and 0.200 mL (2.5 mmol) of 2-butyne and heated at reflux for 4 h. The orange yellow reaction mixture was filtered, rotary evaporated, taken up in minimum methylene chloride, and purified by thin layer chromatography using 1:4 methylene chloride:hexanes as eluent. Two main bands were eluted: the first contained 10 mg of recovered **2** and the second orange band contained 10 mg (35%) of $\text{Ru}_3(\text{CO})_8(\mu_3\text{-}\eta^2\text{-}\text{C}=\text{N}(\text{CH}_2)_3)(\mu\text{-}\eta^2\text{-}\text{CH}_3\text{C}=\text{C}(\text{H})\text{CH}_3)$ (**6**).

Analytical and Spectroscopic Data for 6. Anal. Calcd for $\text{C}_{16}\text{H}_{13}\text{NO}_8\text{Ru}_3$: C, 29.91; H, 2.04; N, 2.18. Found: C, 29.61; H, 2.08; N, 2.28. IR ($\nu(\text{CO})$, hexane): 2079 (m), 2059 (s), 2048 (s), 2024 (m), 2004 (vs), 1963 (w), 1941 (m, br) cm^{-1} . $^1\text{H-NMR}$ (CDCl_3 , 400 MHz): 3.57 (m, 1H), 3.34 (m, 1H), 3.13 (m, 1H), 2.66 (m, 1H), 2.34 (s, 3H), 2.16 (q, 1H), 2.04 (d, 3H), 1.63 (m, 1H), 1.26 (m, 1H) ppm.

Synthesis of $\text{Os}_3(\text{CO})_9(\text{C}=\text{N}(\text{CH}_2)_3)(\text{CH}_3\text{C}=\text{C}(\text{H})\text{CH}_3)$ Isomeric Mixture (8** and **9**) and $\text{Os}_3(\text{CO})_8(\mu_3\text{-}\eta^2\text{-}\text{C}=\text{N}(\text{CH}_2)_3)(\mu\text{-}\eta^2\text{-}\text{CH}_3\text{C}=\text{C}(\text{H})\text{CH}_3)$ (**10**).** Compound **7a** (110 mg, 0.12 mmol) was combined with 20 mL of CH_2Cl_2 and 10 mL of CH_3CN . Trimethylamine *N*-oxide (14 mg, 0.18 mmol) in 20 mL of acetonitrile was added dropwise and the reaction solution stirred for 1 h. The deep yellow solution was filtered through a short florisil column and rotary evaporated to yield a yellow oil. A solution of 47 μL of 2-butyne (0.60 mmol) in 20 mL of CH_2Cl_2 was added dropwise and the red-orange solution stirred for 1 h. The solution was then rotary

evaporated and purified by thin layer chromatography using 1:4 methylene chloride/hexanes as eluent. Two major bands were eluted: the faster moving yellow band contained 62 mg (55%) of $\text{Os}_3(\text{CO})_9(\text{C}=\text{N}(\text{CH}_2)_3)(\text{CH}_3\text{C}=\text{C}(\text{H})\text{CH}_3)$ (**8** and **9**), and the slower moving orange band contained 21 mg (19%) of $\text{Os}_3(\text{CO})_8(\mu_3\text{-}\eta^2\text{-}\text{C}=\text{N}(\text{CH}_2)_3)(\mu\text{-}\eta^2\text{-}\text{CH}_3\text{C}=\text{C}(\text{H})\text{CH}_3)$ (**10**).

Analytical and Spectroscopic Data for 8 and 9. IR ($\nu(\text{CO})$, hexane): 2104 (w), 2092 (m), 2071 (s), 2064 (s), 2054 (s), 2045 (s), 2038 (s), 2022 (s), 1992 (s, br), 1974 (s, br), 1966 (s, br), 1941 (w) cm^{-1} . $^1\text{H-NMR}$ (CDCl_3 , 400 MHz) mixture of **8** and **9** of equal relative intensity: 6.90 (q, 1H), 3.93 (q, 1H), 3.90–3.45 (multiplets, $\sim 4\text{H}$), 3.14 (m, 0.6H), 2.99 (s, 3H), 2.87 (m, 1H), 2.58 (m, 2H), 2.39 (s, 3H), 2.29 (d, 3H), 2.10 (d, 3H), 1.76 (m, 1H) ppm. Not all of the methylene resonances could be assigned due to overlap. Other methyl doublets of lower relative intensity were observed at 2.14 and 2.24 ppm.

Analytical and Spectroscopic Data for 10. Anal. Calcd for $\text{C}_{16}\text{H}_{13}\text{O}_8\text{NOs}_3$: C, 20.92; H, 1.41; N, 1.52. Found: C, 21.11; H, 1.39; N, 1.57. IR ($\nu(\text{CO})$, hexane): 2079 (m), 2059 (s), 2048 (s), 2024 (m), 2004 (vs), 1963 (w), 1941 (m, br) cm^{-1} . $^1\text{H-NMR}$ (CDCl_3 , 400 MHz): 4.10 (q, 1H), 3.30 (dd, 1H), 2.98 (m, 3H), 2.76 (s, 3H), 2.31 (d, 3H), 1.82 (m, 1H), 1.43 (m, 1H) ppm. $^{13}\text{C-NMR}$ (CDCl_3 , 100 MHz) carbonyl region: 186.19, 185.96, 185.58, 180.27, 178.24, 177.56, 176.23, 175.74 ppm; hydrocarbon region: 73.14 (CH_2), 62.96 (CH_2), 51.55 (CH), 36.13 (CH_2), 25.34 (CH_3), 19.10 (CH_3) ppm. Thermolysis of the yellow band containing **8** and **9** in refluxing heptane led to conversion to **10** in about 90% yield after recrystallization.

Synthesis of $\text{Os}_3(\text{CO})_8(\mu_3\text{-}\eta^2\text{-}\text{C}=\text{N}(\text{CH}_2)_3)(\mu\text{-}\eta^2\text{-}\text{C}_6\text{H}_5\text{C}=\text{C}(\text{H})\text{C}_6\text{H}_5)$ (11**).** A procedure identical to that described for the preparation of **10** was used for the synthesis of **11** except that the orange and yellow bands obtained from the reaction were combined and thermolyzed directly to yield 20 mg (30%) of $\text{Os}_3\text{CO}_8(\mu_3\text{-}\eta^2\text{-}\text{C}=\text{N}(\text{CH}_2)_3)(\mu\text{-}\eta^2\text{-}\text{C}_6\text{H}_5\text{C}=\text{C}(\text{H})\text{C}_6\text{H}_5)$ (**11**) from 58 mg of **7a**. Somewhat lower yields were obtained by heating **3** with excess diphenylacetylene in refluxing heptane.

Analytical and Spectroscopic Data for 11. Anal. Calcd for $\text{C}_{26}\text{H}_{17}\text{NO}_8\text{Os}_3$: C, 30.00; H, 1.63; N, 1.34. Found: C, 30.16; H, 1.82; N, 1.42. IR ($\nu(\text{CO})$, hexane): 2077 (m), 2048 (s), 2028 (m), 2004 (vs), 1982 (m), 1962 (w), 1944 (m, br) cm^{-1} . $^1\text{H-NMR}$ (CD_2Cl_2 , 400 MHz): 7.45–6.84 (mm, 10H), 4.84 (s, 1H), 3.57 (m, 1H), 3.12 (m, 2H), 2.91 (m, 1H), 1.88 (m, 1H), 1.39 (m, 1H) ppm.

Synthesis of $\text{Os}_3(\text{CO})_9(\mu\text{-}\eta^2\text{-}\text{C}=\text{N}(\text{CH}_2)_3)(\mu_3\text{-}\eta^3\text{-}\text{CH}_3\text{O}_2\text{-CC}=\text{C}(\text{H})\text{CO}_2\text{CH}_3)$ (12**).** This complex could be prepared by the procedure outlined for the preparation of **8**, **9**, and **10** above. By this procedure, 36 mg (71%) of **12** was obtained from 45 mg of **7b**. Refluxing 42 mg of **3** in the presence of a 5-fold excess of dimethylacetylenedicarbonate in heptane yields 21 mg (43%) of **12**.

Analytical and Spectroscopic Data for 12. Anal. Calcd for $\text{C}_{19}\text{H}_{13}\text{O}_{13}\text{NOs}_3$: C, 22.07; H, 1.25; N, 1.35. Found: C, 21.96; H, 1.18; N, 1.47. IR ($\nu(\text{CO})$, hexane): 2084 (m), 2058 (s), 2034 (s), 2009 (s), 1998 (m, br), 1980 (m, br), 1963 (w, br) cm^{-1} . $^1\text{H-NMR}$ (CDCl_3 , 400 MHz): 3.73 (s, 3H), 3.65 (s, 3H), 3.37 (m, 2H), 2.67 (s, 1H), 2.36 (t, 2H), 1.53 (m, 2H) ppm. $^{13}\text{C-NMR}$ (CDCl_3 , 100 MHz) carbonyl region: 187.62, 186.27, 184.89, 184.79, 184.58, 180.24, 180.24, 175.41, 175.06, 174.25 ppm; hydrocarbon region: 197.9 ($\text{C}=\text{N}$), 173.05 (CO_2Me), 70.45 (CH_2), 54.99 (CH), 53.87 (CH_2), 52.05 (CH_2), 40.76 (CH_3), 23.71 (CH_3) ppm.

Synthesis of $\text{Os}_3(\text{CO})_8(\mu\text{-}\eta^6\text{-}(\text{CH}_3\text{C}(\text{H})=\text{C}(\text{CH}_3)\text{C}(\text{CH}_3)=\text{C}(\text{CH}_3)\text{C}=\text{N}(\text{CH}_2)_3))$ (13**).** Compound **7a** (35 mg, 0.038 mmol) was dissolved in 30 mL of methylene chloride and then 12 mg (0.10 mmol) of trimethylamine *N*-oxide dihydrate and 50 μL (0.61 mmol) of 2-butyne were added. The reaction mixture was stirred at room temperature for 2 h, and the solvent was evaporated under vacuum and the residue purified by thin layer chromatography using hexane/ CH_2Cl_2 (10:3) as eluent. Two bands were eluted: a yellow band which proved to be unreacted **7a** (10 mg), and 7 mg (19%) of **13**.

Analytical and Spectroscopic Data for 13. Anal. Calcd for $\text{C}_{20}\text{H}_{19}\text{O}_8\text{NOs}_3$: C, 24.70; H, 1.95; N, 1.44. Found: C, 24.98;

H, 1.84; N, 1.41. IR ($\nu(\text{CO})$, hexane): 2075 (m), 2006 (sh), 1999 (s), 1986 (m, br), 1943 (w), 1916 (w, br) cm^{-1} . $^1\text{H-NMR}$ (CDCl_3 , 400 MHz) 4.04 (m, 1H), 3.07 (m, 1H), 2.91 (m, 2H), 2.33 (s, 3H), 2.15 (s, 3H), 2.09 (d, 3H), 2.05 (s, 3H), 1.95 (m, 1H), 1.76 (m, 1H), 1.75 (q, 1H) ppm.

X-ray Structure Determination of 5, 11, 12, and 13. Crystals of **5**, **11**, **12**, and **13** for X-ray examination were obtained from saturated solutions of each in hexane/dichloromethane solvent systems at $-20\text{ }^\circ\text{C}$. Suitable crystals of each were mounted on glass fibers, placed in a goniometer head on the Enraf-Nonius CAD4 diffractometer, and centered optically. Unit cell parameters and an orientation matrix for data collection were obtained by using the centering program in the CAD4 system. Details of the crystal data are given in Table 1. For each crystal, the actual scan range was calculated by scan width = scan range + $0.35 \tan \theta$, and backgrounds were measured by using the moving-crystal/moving-counter technique at the beginning and end of each scan. Two representative reflections were monitored every 2 h as a check on instrument and crystal stability, and an additional two reflections were monitored periodically for crystal orientation control. Lorentz, polarization, and decay corrections were applied, as was an empirical absorption correction based on a series of ψ scans for each crystal. The weighting scheme used during refinement for all structures was $1/\sigma^2$.

Each of the structures was solved by the Patterson method using SHELXS-86,¹⁵ which revealed the positions of the metal atoms. All other non-hydrogen atoms were found by successive difference Fourier syntheses. Hydrogen atoms were included for each structure, placed in their expected chemical positions using the HFIX command in SHELXL-93,¹⁶ and included as riding atoms in the final least squares refinements with U_s

which were related to the atoms ridden upon. All other non-hydrogen atoms were refined anisotropically.

Scattering factors were taken from Cromer and Waber.¹⁷ Anomalous dispersion corrections were those of Cromer.¹⁸ All data processing for **11** and **13** was carried out on a DEC Micro VAXII using the MolEN programs and for **5** and **12** on a DEC 3000 AXP computer using the Open MolEN system of programs.¹⁹ Structure refinement and preparation of figures and tables for publication were carried out on a DEC Micro VAXII using MolEN for **11** and **13** and on PC's using SHELXL-93¹⁶ and XP/PC²⁰ programs for **5** and **12**.

Acknowledgment. We gratefully acknowledge the support of the National Science Foundation (CHE9319062 and 9624367, E.R.), Consiglio Nazionale delle Ricerche (L.M.), the Ministry of University and Scientific Research (L.M.), the University of Montana (E.R.), and the Università di Torino (E.R.) for support of this research.

Supporting Information Available: Complete distances and bond angles, anisotropic thermal parameters, and atomic coordinates, (Tables 6–19) for **5**, **11**, **12**, and **13** (28 pages). Ordering information is given on any current masthead page.

OM9610915

(16) Sheldrick, G. M. *Program for Structure Refinement*; University of Goettingen: Goettingen, Germany, 1993.

(17) Cromer, D. T.; Waber, J. T. *International Tables for X-ray Crystallography*; Kynoch: Birmingham, 1974; Vol. 4, Table 2.2B.

(18) Cromer, D. T. *International Tables for X-ray Crystallography*; Kynoch: Birmingham, 1974; Vol. 4, Table 2.3.1.

(19) Fair, C. Kay, "MolEN" *Structure Determination System*; Enraf-Nonius: Delft, The Netherlands, 1990.

(20) "XP/PC" *Molecular Graphics Software*; Siemens Analytical X-ray Instruments, Inc.: Madison, WI.

(15) Sheldrick, G. M. *Acta Crystallogr.* **1990**, *A46*, 467.